# Physical Origin of General Oscillation of Structure, Surface Energy, and Electronic Property in Rutile TiO$_2$ Nanoslab

T. He, J. L. Li, and G. W. Yang*

State Key Laboratory of Optoelectronic Materials and Technologies, Institute of Optoelectronic and Functional Composite Materials, Nanotechnology Research Center, School of Physics and Engineering, Sun Yat-sen University, Guangzhou 510275, Guangdong, P. R. China

ABSTRACT: Titanium oxide (TiO$_2$) nanostructures have been attracting consistent focus in the past few years because of their enhanced power in solar-energy conversion. Surface and interface play a crucial role in the determination of thermodynamic stability and electronic structure of TiO$_2$ nanostructures. The rutile (110) nanoslab (NS) has been used as a common subject to investigate the surface relaxation, defect characters, molecule adsorption, and chemically dynamic reaction of TiO$_2$ nanostructures. Up to date, a long-time standing issue in TiO$_2$ NS, i.e., the general oscillation of structure, surface energy and electronic property with changing of NS thickness, has not

been clear. We have presented a comprehensive investigation on the relationship between surface and oscillation behavior in the TiO$_2$ (110) NS by the first-principles calculations accompanied with the wave function analysis. We clearly, for the first time, pointed out that the dipoles and surface states bonding induced by the surface−surface interactions are the physical origin of general oscillations in the TiO$_2$ (110) NS. Our findings not only have a new insight into the basic interactions between surfaces in TiO$_2$ nanostructures, but also provide useful information for tuning the photocatalytic and photovoltaic properties by surface design.

KEYWORDS: TiO$_2$ nanoslab, first-principles, oscillation, surface energy, band gap, surface−surface interaction
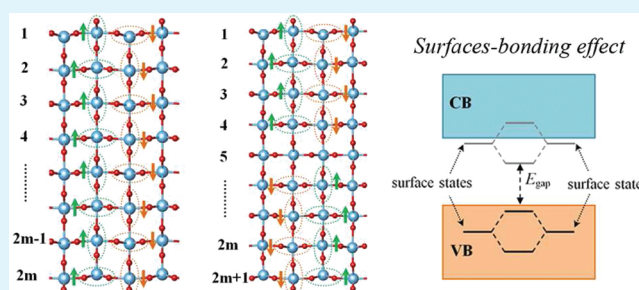
1. INTRODUCTION

Titanium dioxide (TiO$_2$) is a versatile material in the fields of solar-energy capture and utilization. The nanostructure forms of TiO$_2$ have been considerably attracting worldwide attentions in the past few years due to their high reactivity and low-cost benefit in solar-energy conversion processes,[1−3] which also present the possibility of tuning the conversion efficiency in future power devices, through either size or morphology control.[1,4−7] It is well-known that the surface of TiO$_2$ nanostructures plays a major role in the determination of their thermodynamic and electronic properties.[7−10] Moreover, surface is the main part in reactions with solar-ray, water, and functional groups. To increase the conversion power of TiO$_2$, it is crucial to increase the surface-to-bulk ratio by decreasing materials size to nanometer, where the internal relation between surfaces becomes fundamental, which tunes the reactivity of nano-TiO$_2$ in both photocatalytic and photovoltaic applications. In this viewpoint, efforts to reveal the relationship among size, surface, and electronic structure of TiO$_2$ nanostructures are in great demand.

As an important prototype of nano-TiO$_2$, the quasi-two-dimensional (Q2D) nanoslab (NS) of rutile TiO$_2$ has been used in theoretically studying the important properties including surface atomic relaxation,[11−15] defect character,[16−19] molecule adsorption,[20−30] and reaction barriers,[25,26] of rutile TiO$_2$ (110) surface. It is not only because TiO$_2$ (110) surface is the most stable one in all low-index surfaces, but also a typical interface

in between semiconducting substrate and active molecules/ groups in liquid environment.[29,30] Abundant theoretical and experimental works have been present probing into the atomic displacement[11−15] and chemical reaction pathway[20,23−26] of pure, reduced, or reconstructed rutile (110) surface. The possibility of tuning the photovoltaic and photocatalytic properties of TiO$_2$ (110) NS through surface/size design, and the interplay between surface and NS thickness, are two important aspects under quantum confinement.[31−33] Although there have been a lot of constructive works, a long-time standing issue in TiO$_2$ NS has not been clear so far, that is the general oscillation of structure, surface energy and electronic structure when the NS thickness is changed.[23,24,34−38] These oscillations have wide impact on the theoretical judgment of chemical reactivity of TiO$_2$ (110) surface. For example, oscillation of surface energy (E_{surf}) affects the thermodynamic stability of TiO$_2$ NS, and oscillating band gap value also suggests a tunable photosensitivity which suggests the importance in fabricating future photoelectric devices based on nano-TiO$_2$. Moreover, these intrinsic oscillations have close relationship with other property oscillations of TiO$_2$ (110) surface, e.g., the adsorption energy,[20−30] work function,[37] and defect formation energy.[39−41]

To date, much few works focusing on the physical origin of general oscillation in TiO₂ (110) NS have been presented. Bredow et al. studied the oscillation of interlayer distance, surface and adhesion energy, and electronic structure in TiO₂ NS.[35] They found the clue of rehybridization of O 2p and Ti 3*d* orbitals affecting the oscillation in NS with odd or even TiO₂ layers, so-called the 'odd−even oscillation'. It is the first time both geometric and electronic factors related with NS symmetry was considered. Mitev et al. have also tried to explain the oscillation in the TiO₂ (110) surface properties in terms of surface lattice dynamics mediating a long-range electrostatic interaction.[38] However, these theories have limits for explaining all the oscillations based on the TiO₂ (110) surface, e.g., adsorption energy, work function, and defect formation energy.[20−30,37,39−41] In fact, the rehybridization of orbitals presents in nearly all the allotropic or size-decreased nanomaterials in certain extent. Why it brings out the intrisic oscillation in TiO₂ (110) NS but not in other nanomaterials, is hard to understand based on the Bredow's work. It is well-known that because of the increasing surface-to-bulk ratio, the surface relaxation should play an important role in nanomaterials. Therefore, a deep understanding of the link between surface relaxation and the general oscillation in the TiO₂ (110) NS is needed in pursuing the physical origin of oscillation. In this contribution, a study focusing on the surface effect on both geometric and electronic structures in TiO₂ NS is in great demand.

For this issue, we perform a comprehensive investigation on the relationship between surface and oscillations in the TiO₂ (110) NS by the first-principles calculations accompanied with the wave function analysis. Importantly, we have had the new physical insight into the general oscillation of structure, surface energy and electronic property with changing the thickness of the TiO₂ (110) NS, based on surface−surface interaction, which is significant for the understanding of the role of surface in TiO₂ nanostructures and provides useful information for designing TiO₂ nanostructures in different applications.

2. METHOD AND COMPUTATION

First-principle calculations are carried out by SIESTA code[42−44] in the framework of density-functional-theory (DFT).[45,46] Norm-conserving pseudopotentials[47−49] and local density approximation (LDA)[50] exchange-correlation functional are adopted. To give an accurate description of geometric and electronic structure, semicore states of Ti atom $(3s^2 3p^6)$ are considered. Numerical electron wave functions are constructed by a double-ζ basis set plus polarization functions (DZP).[51] All numerical integrals are performed on a real space grid with an equivalent energy cutoff of 150 Ry. The Brillouin zone is sampled by a dense Monkhorst-Pack $6 \times 10 \times 1$ k-mesh.[52] To exclude the instantaneous interaction between images with other artificial effects, a vacuum space of at less 25 Å and a slab dipole correction are adopted in our periodic DFT calculations. Total energy is calculated in precision of 10^{-4} eV. Equilibrium structure is obtained by fully atomic relaxation in the conjugate gradient (CG) algorithm when all Hellmann−Feynman forces are less than 0.01 eV/Å. This setting gives the equilibrium lattice parameters a (4.555 Å) and c (2.933 Å) of bulk rutile TiO₂, agreeing well with the experiment (a = 4.594 Å and c = 2.959 Å)[53] and other theoretical works.[54−56]

3. RESULTS AND DISCUSSION

Before probing into the interaction in the TiO₂ (110) NS, we first study the geometry and electronic structure of an approximately isolated surface in a thick NS without the internal surface−surface interaction. After structure optimization, we find that a NS containing 25 TiO₂ layers (8 nm thick) gives

well-converged surface relaxation and band gap value (1.65 eV), as shown in oanels a and b in Figure 1 for the unrelaxed and
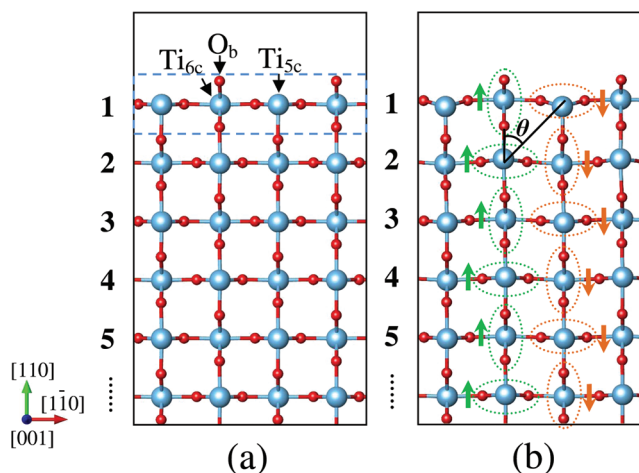

Figure 1. Structures of (a) unrelaxed and (b) relaxed rutile (110) surfaces for a 25-layers NS. A TiO₂ layer is marked in a blue dash box. Ti and O atoms are plotted as big blue and small red balls, respectively. Local dipoles (p_{out} and p_{in}) are plotted in dot ellipses with an arrow (↑ or ↓) denoting the direction.

relaxed surface, respectively. The clean rutile (110) surface has two low-coordinated species, i.e., the 5-fold-coordinated Ti atom (Ti$_{5c}$), and the 2-fold-coordinated O atom (O$_b$) bridging on other two 6-fold-coordinated Ti atoms (Ti$_{6c}$), as shown in Figure 1. The surface atoms are fully relaxed compared with the bulk lattice, seeing Figure 1(b), which has been revealed by abundant theoretical and experimental works.[11−15] The O$_b$ becomes close to the Ti$_{6c}$ with the O$_b$-Ti$_{6c}$ bond-length shorten by 7.2%, and the Ti$_{5c}$ relaxes into the surface with a displacement of 0.456 Å in $[\overline{1}10]$ direction. These results agree well with the photoelectron diffraction and low-energy electron diffraction experiments.[14] By minimizing the surface dangling bonds of the O$_b$ and Ti$_{5c}$ atoms, their relaxation is favorable in decreasing the surface energy.

An interesting character of the TiO₂ (110) surface structure is the oscillation of interlayer spacing,[35] which is defined as the distance in $[110]$ direction between the averaged positions of two TiO₂ trilayers, as shown in Figure 1a. The oscillation with increasing the depth, or the TiO₂ layer number (L), can be found in Figure 2a. On the basis of the relaxation of surface O$_b$ and Ti$_{5c}$, we propose a totally new mechanism for the changes of interlayer spacing, which originates from two oppositely polarized surface dipoles induced by the relaxations of anion O$_b$ and cation Ti$_{5c}$ in the surface, as shown in Figure 1b. Mulliken population analysis reveals that, the outward polarized TiO₂ unit (p_{out}) around O$_b$ and the inward polarized TiO₂ unit (p_{in}) around Ti$_{5c}$ carry local dipole moments of 2.34 D and −2.34 D, respectively, where the $[110]$ direction is defined as the positive direction. These two surface dipoles induce a series of local dipoles under the first TiO₂ layer, which fast decay to less than 0.1 D (absolute value) when $L > 9$, as shown in Figure 1b and Figure 2b. The parallel dipoles will interact electrostatically with each other, and the dipole−dipole interaction energy (U_i) can be described in the form of

$$U_i = \pm \frac{p_1 p_2}{4\pi\varepsilon r_{12}{}^3}(1 - 3\cos^2\theta)$$

(1)

(a)

(b)
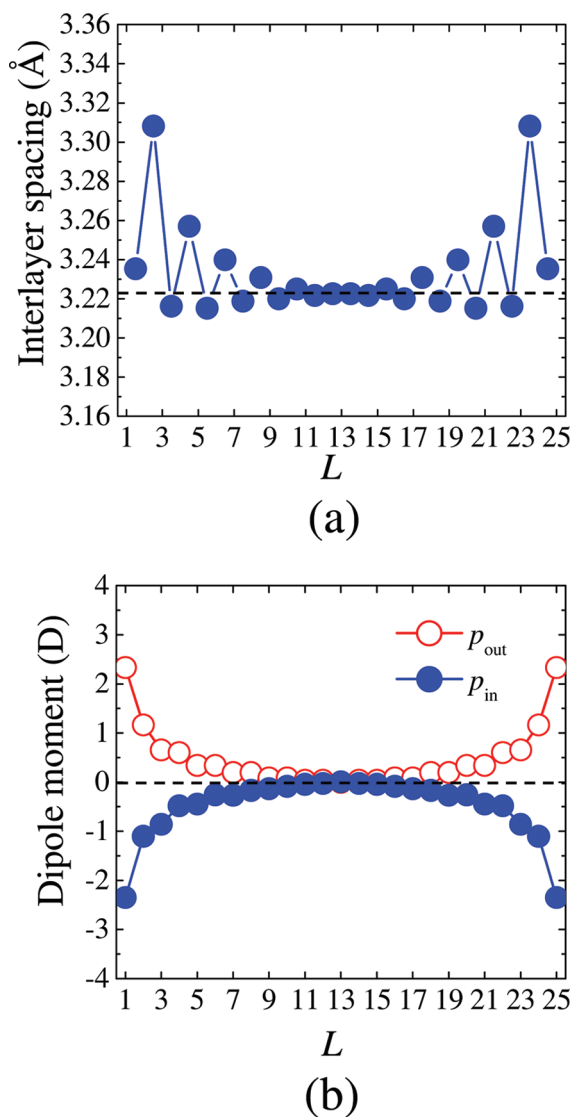
Figure 2. Oscillation of (a) interlayer spacing and (b) local dipole moments in a 25-layers NS versus layer number (L). Dash lines indicate the converged values.

where the first + (or −) sign denotes the interaction between the same (or opposite) polarized dipoles $\vec{p_1}$ and $\vec{p_2}$, ε is the dielectric constant, r_{12} refers to the distance between the center of two dipoles, and θ is the angle between $\vec{p_1}$ and $\vec{r_{12}}$ as shown in Figure 1b. According to eq 1, the interaction between diagonal p_{in} and p_{out} (seeing Figure 1b) will enlarge the θ to lower down the U_i. It gives rise to a puckered surface where all the Ti atoms in p_{in} and those in p_{out} are not in the same (110) planes but have a small displacement, and the first and the second TiO$_2$ layers get close to form a compact double-layer, and so forth, as shown in Figure 1b. However, the puckering also increases the surface instability. In order to effectively buffer this lattice instability, the interlayer spacing between the second layer and the third TiO$_2$ layer is enlarged. Thus the interlayer spacing oscillates with the increasing of L. Note that, the local dipoles of (110) surface mostly come from the intrinsic relaxations of Ti$_{5c}$ and O$_b$ but depend less on the charge population scheme used. We also perform Bader population analysis[57] to calculate the charge transfer, but no fundamental difference is found. We conclude that the mechanism of local dipoles in inducing the interlayer-spacing oscillation is intrinsic.

Not only the surface geometry but also the electronic structure has close relationship with local dipoles in TiO$_2$ (110) surface. We calculate the energy band structure of surface as shown in Figure 3(a), where the bands of bulk rutile TiO$_2$ are

(a)

(b)
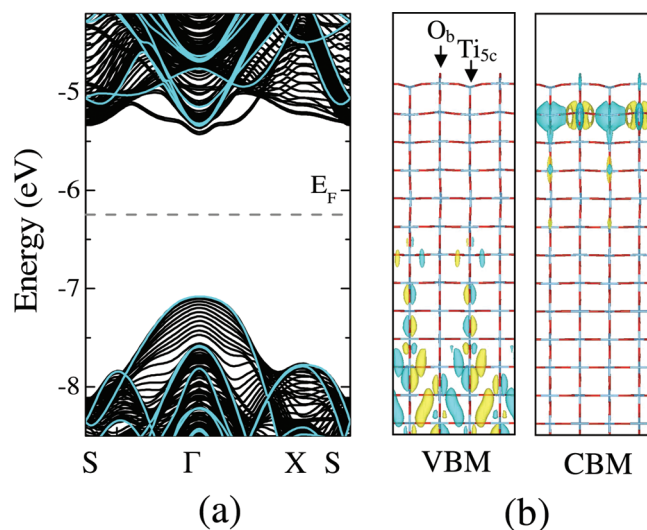
Figure 3. (a) Energy band structure and (b) VBM/CBM wave function iso-surfaces of a 25-layers NS. The energy bands of bulk TiO$_2$ are plotted in cyan (gray) for comparison. The iso-surface level is 0.1.

also plotted in light lines for comparison. Two degenerated unoccupied bands and a series of degeneracy-removed occupied bands are found around Fermi-level (E_F) of NS, both lower than the conduction band minimum (CBM) and the valence band maximum (VBM) of bulk TiO$_2$. These surface states are further evidenced by the distribution of the CBM wave functions on subsurface as well as the bulk characters of the VBM wave functions shown in Figure 3(b). Why do the surface states shift downward compared with the bulk bands? Note that, the p_{in} in the first TiO$_2$ layer has a displacement of about 0.25 Å in $[\overline{1}10]$ direction from the p_{out} as discussed above. This displacement induces a net built-in electric field along $[\overline{1}10]$, which decays with the depth. Consequently, the energy bands close to the surface are bended down from those of bulk, as illustrated by Figure 4.
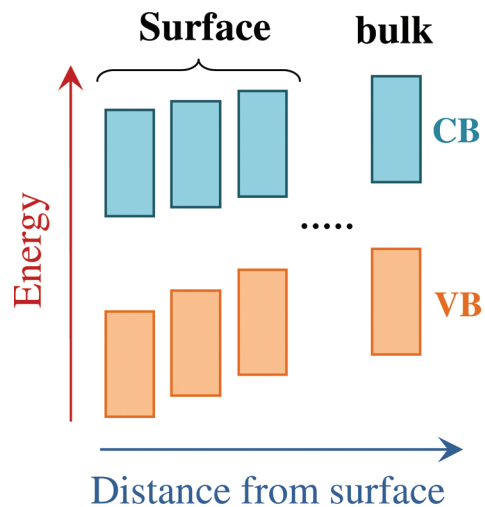
Figure 4. Schematic diagram of energy band bending near the surface under built-in electric field induced by surface dipoles.

2194

dx.doi.org/10.1021/am300193d | ACS Appl. Mater. Interfaces 2012, 4, 2192–2198

We find that the bending of surface conduction band is not as remarkable as that of valence band, which is mostly because that the highly electronegativity of O atoms in TiO$_2$ surface restricts the relaxation of the occupied O $2p$ orbitals and gives rise to more dispersive energy levels under the CBM (Figure 3a). We note that, the spatial separation of CBM and VBM should facilitate the charge separation in TiO$_2$ (110) surface for photocatalytic applications. Moreover, the dependence of electronic structure on local dipoles implies that changing the surface dipoles, e.g., by surface reduction or decorations, will definitely tune the photosensitivity of a TiO$_2$ (110) surface. It provides a new insight into the important role of surface design in obtaining a high-efficiency photocatalytic TiO$_2$ surface.[16−19]

On the basis of the picture of local dipoles and the electronic structure of TiO$_2$ (110) surface, the oscillations in a TiO$_2$ (110) NS with shortened surface−surface distance and the pronounced surface−surface interaction can be addressed. To eliminate the artificial effect from neighboring images in periodic DFT, a large vacuum space of >25 Å was employed, which can well promise the effectiveness of results. The TiO$_2$ (110) NS is classified into two categories according to surface symmetries,[35] one of which consists of even number of TiO$_2$ layers with asymmetric surfaces (NS$_{2m}$) and another has odd layers with symmetric surfaces (NS$_{2m+1}$), as shown panels in a and b in Figure 5.
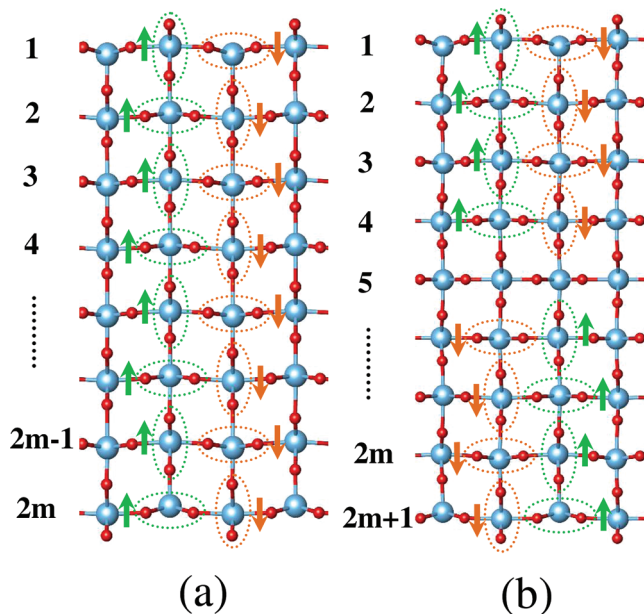
Figure 5. Relaxed structures of NS$_{2m}$ and NS$_{2m+1}$. Local dipoles (p_{out} and p_{in}) are plotted in dot ellipses with an arrow (↑ or ↓) denoting their directions.

As we have discussed above, the dipoles from one surface will attract (or repel) those from the opposite surface for the asymmetric (or symmetric) surface−surface pair, which will increase (or decrease) the stability of NS$_{2m}$ (or NS$_{2m+1}$). This difference of stability in NS$_{2m}$ and NS$_{2m+1}$ can be well-understood by calculating the surface energy (E_{surf}), in terms of

$$E_{surf} = \frac{1}{2}(E_{NS} - n\mu)/S \qquad (2)$$

where E_{NS} and n denote the total energy and the number of TiO$_2$ units in the NS$_N$ ($N = 2m$ or $2m+1$, m is an positive integer), μ is the chemical potential of a TiO$_2$ unit in bulk, and

S refers to the unit cell surface area. The curves of E_{surf} versus slab thickness are plotted in Figure 6a. It is found that the E_{surf} oscillates between NS$_{2m}$ and NS$_{2m+1}$ with a hierarchy of $E_{surf,2m} < E_{surf,2m+1}$, and converges to ~0.61 eV/Å^2 for the NS$_N$ with $N > 13$, agreeing well with other theoretical works.[34−38] This oscillation proves our speculation of the surface−surface interaction in TiO$_2$ (110) NS, and evidence the local dipoles.

The direct relation between surface energy and local dipoles interaction can be also found in Figure 6b, where the surface p_{in} and p_{out} and the internal p_{in} in NS$_{2m}$ and NS$_{2m+1}$ vary with NS thickness. For NS$_{2m+1}$, the internal dipole moment of p_{in} converges to nearly zero when $N = 13$, which is coincident with the quench of E_{surf} oscillating amplitude when $N = 13$ as shown in Figure 6a. It proves that the oscillation of surface energy is directly related to the surface−surface interaction in language of local dipoles. We also find the internal p_{in} in NS$_{2m}$ in fact does not converge to zero as the surface p_{in}/p_{out} at $N = 14$, as shown in Figure 6b. In NS$_{2m}$, the virtual convergence of surface energy at $N = 14$ is because of the compensation of surface attraction with upgraded lattice instability when the local dipoles begin to interact with each other in NS$_{2m}$. From this viewpoint, NS$_{2m+1}$ with fast convergence of both surface energy and local dipoles should be more representative and economical in modeling an isolated TiO$_2$ (110) surface than NS$_{2m}$. Because we have excluded the artificial effect from periodic images, this internal interaction between two surfaces is an intrinsic property in NS.

Not only the local dipoles have effect on surface−surface interaction, but also the interaction changes the surface dipoles for NS$_{2m}$ and NS$_{2m+1}$, as shown in Figure 6b. In NS$_{2m}$, the surface attraction reduces the U_i but increases the absolute values of surface p_{in} and p_{out}. On the other hand, surface dipoles are suppressed in the NS$_{2m+1}$ due to surface−surface repulsion and increased U_i. We find that the sensitivity of p_{in} in surface is much higher than that of p_{out} in both NSs, illustrated by the slower convergence of p_{in} (at $N = 9$) than p_{out} (at $N = 4$), because of the higher mobility of Ti$_{5c}$ than O$_b$. These features shed light on the well-known oscillation of adsorption energy (E_{ads}) when a molecule/group is adsorbed on a clean TiO$_2$ (110) surface.[20−30] The adsorption energy is defined as the difference between total energy of water-adsorbed TiO$_2$ (110) surface and the sum of the energies of clean surface and a water molecule. Take the case of adsorption of water molecule for example, the polar H$_2$O could anchor at either Ti$_{5c}$ or O$_b$ site, which have sensitive dipole moments to NS thickness. Thus the increased (or decreased) surface dipole moments in NS$_{2m}$ (or NS$_{2m+1}$) shows a stronger (or weaker) electrostatic attraction between water and template NS. Moreover, the charge transfer and the bonding strength between H$_2$O and NS are different for NS$_{2m}$ and NS$_{2m+1}$ due to different charge population of surface dipoles. Consequently, the adsorption energy oscillates between NS$_{2m}$ and NS$_{2m+1}$ with changing the NS thickness. Furthermore, our results are fully supported by the proposal of Harris et al.[23] that the dissociation of H$_2$O on TiO$_2$ (110) surface has highly dependence on slab thickness. It is because the error of dissociation of H$_2$O (in form of OH$^-$ and H$^+$) on Ti$_{5c}$ and O$_b$ sites is raised up, considering the sensitivity difference of p_{in} and p_{out}, particularly when $N < 9$. Note that, based on the picture of surface−surface interaction, a series of energy-related oscillations in TiO$_2$ (110) surface, e.g., the work function[37] and the defect formation,[39−41] can be clarified.

How does the surface−surface interaction influence the electronic structure of a TiO$_2$ NS? We calculate the band gap
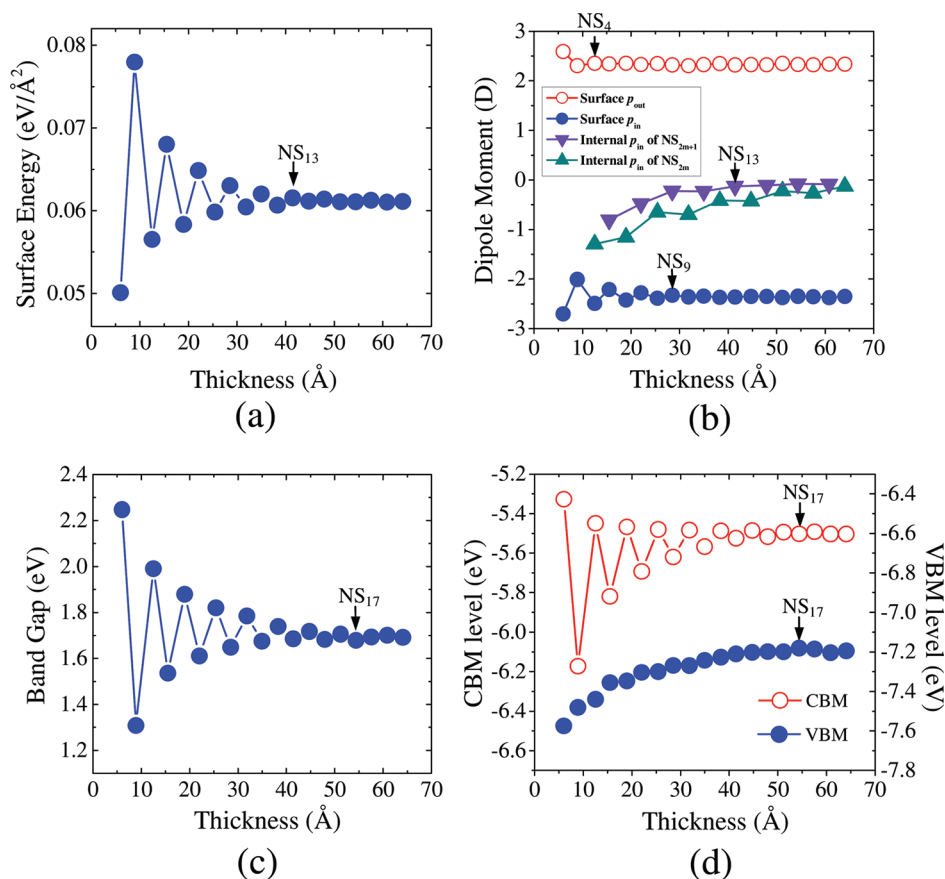
Figure 6. (a) Surface energy, (b) dipole moments in surface and near the NS center, (c) band gap value, and (d) CBM/VBM levels of a series of NS_N ($2 \leq N \leq 20$).

value (E_{gap}) of a series of NS_N ($2 \leq N \leq 20$), and find that E_{gap} also oscillates between NS_{2m} and $NS_{2\,m+1}$, known as 'odd−even oscillation',[34−38,58] as shown in Figure 6c. The E_{gap} of NS_{2m} (or NS_{2m+1}) decreases (or increases) when the slab thickness is increased. To understand this oscillation, it is better to separately consider the variation of CBM and VBM energy levels.[35] As shown in Figure 6d, we find a synchronous oscillation of CBM as E_{gap}, and a monotonic decrease of VBM, with decreasing of thickness. The oscillation of CBM does not follow the well-known monotonic variation of energy level under quantum-confinement effect (QCE). This distinct behavior has close relationship with the interaction of surface states between two opposite surfaces. Taking NS_{10} and NS_{11} for examples, as shown in Figure 7, the VBM of both NS_{2m} and NS_{2m+1} have characteristics of bulk O 2p orbital (left panels in c and d in Figure 7). However, the CBM distribution is different for NS_{2m} and NS_{2m+1}, seeing the right panels of c and d in Figure 7, where the CBM states in NS_{2m} are mainly contributed by separated Ti 3d orbitals localized on distant subsurfaces, but they overlap and bond with each other in NS_{2m+1}. This new bonding in NS_{2m+1} suggest that, the CBM downshift and the band gap narrowing should come from the high kinetic energy of Ti 3d orbitals, the favorable bonding angles, and the large orbital overlapping in NS_{2m+1} with symmetric surfaces. Thus it gives rise to the odd−even oscillation between NS_{2m} and NS_{2m+1}. The effect of bonding between different surface states should be called as the surface-bonding effect (SBE), competing with the conventional quantum-confinement effect (QCE) in decreasing the band gap in NS_{2m+1}, which can be better understood by the illustrative picture of Figure 8. On the

other hand, the high built-in electric field induced by surface−surface attraction, the unfavorable bonding angle, and the less overlapping all restrict the surface-bonding in NS_{2m}. It explains the nonbonding and localization of CBM states in NS_{2m} shown in Figure 7(c).

Note that our theory based on the local dipoles and surface bonding effect fully supports the findings by Bredow et al. of the oscillations in interlayer distance, surface energy, and electronic structure.[35] In our opinion, the rehybridization of O 2p and Ti 3d orbitals described in their work is an intermediate effect in the local dipoles interaction and surface bonding. Meanwhile, our findings directly links to the relaxation of low-coordinated Ti_{5c} and O_b in minimizing the surface dangling bonds, which is fundamental. Moreover, it explains all the other oscillations reported in literatures about the TiO_2 (110) NS/surface, including the well-known oscillation of water-molecules adsorption energy and the uncertainty of water dissociation on a clean TiO_2 (110) surface.[34−38,58] For the oscillation of electronic structure, the role of bonding between surface states is clarified for the first time, which is different from interactions in an isolated (110) surface. Importantly, our findings of the bonding/nonbonding nature of the TiO_2 (110) surfaces hint that, in a quasi-two-dimensional system, the surfaces are atom-like for internal interactions. These findings not only complement the understanding of the fundamental interactions and properties in low-dimensional materials, but also have directive significance for utilizing the surface-bonding effect in designing low-dimensional materials with tuned band gaps for photovoltaic and photocatalytic applications.
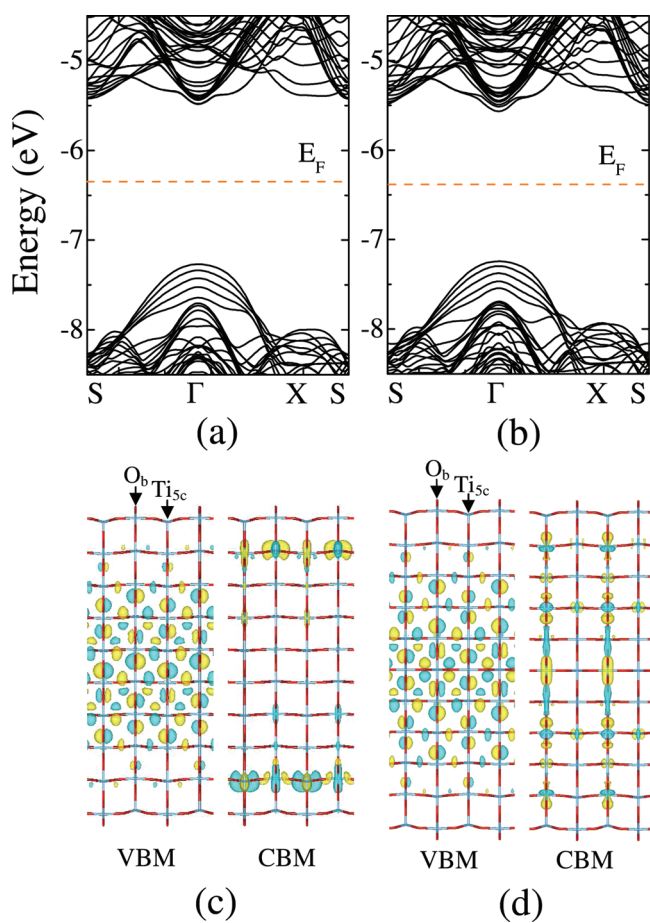
Figure 7. Energy band structures (up) and VBM/CBM wave function iso-surfaces (down) of NS$_{10}$ (left) and NS$_{11}$ (right). The iso-surface level is 0.1.
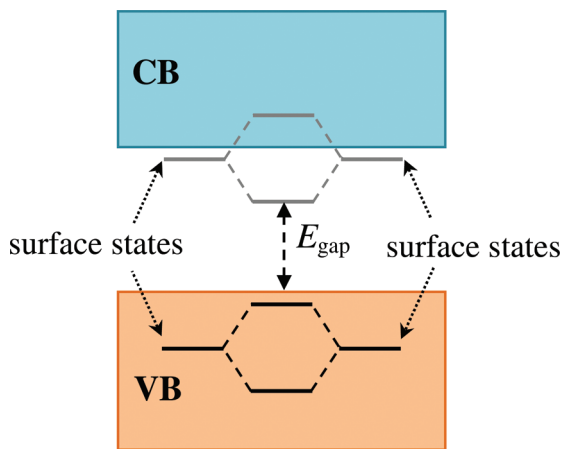
Figure 8. Schematic diagram of surface-bonding effect (SBE) in narrowing band gap.

4. CONCLUSION

We have comprehensively studied the structure and electronic properties of both the isolated TiO$_2$ (110) surface and the quasi-two-dimensional TiO$_2$ (110) nanoslab by the first-principles calculations accompanied with wave function analysis. The long-time standing issue, a general oscillation of structure, surface energy and electronic property in the TiO$_2$ (110) surface and NS are quantitatively pursued by considering

surface dipoles and surface–surface interactions. Theoretical results showed that the relaxation of surface low-coordinated atoms (O$_b$ and Ti$_{5c}$) gives rise to oppositely polarized TiO$_2$ dipoles on the (110) surface, which further induces a series of local dipoles deep into bulk. The dipole–dipole interaction takes responsibility for the oscillation of both interlayer spacing and adsorption energy of the TiO$_2$ (110) surface. When two surfaces are close in a TiO$_2$ (110) NS, internal surface–surface interaction increases (or decreases) the surface stability of the NS containing even (or odd) TiO$_2$ layers, and gives rise to bonding/nonbonding nature of surface states, which well-explains the oscillations of surface energy and band gap values. The surface bonding/nonbonding suggested that, in a nanoslab system, the surfaces are atom-like. Our findings complement the understanding of the basic interactions in low-dimensional materials and shows the significance of surface design in exploiting potential photovoltaic and photocatalytic nanomaterials.

■ AUTHOR INFORMATION

Corresponding Author
*E-mail: stsygw@mail.sysu.edu.cn.

Notes
The authors declare no competing financial interest.

■ REFERENCES

(1) Feng, X. J.; Shankar, K.; Varghese, O. K.; Paulose, M.; Latempa, T. J.; Grimes, C. A. *Nano Lett.* **2008**, *8*, 3781.
(2) Lu, W.; Xiang, J.; Timko, B. P.; Wu, Y.; Lieber, C. M. *Proc. Natl. Acad. Sci. U.S.A.* **2005**, *102*, 10046.
(3) Baik, J. M.; Kim, M. H.; Larson, C.; Chen, X.; Guo, S.; Wodtke, A. M.; Moskovits, M. *Appl. Phys. Lett.* **2008**, *92*, 242111.
(4) Li, C.; Sato, R.; Kanehara, M.; Zeng, H.; Bando, Y.; Teranishi, T. *Angew. Chem., Int. Ed.* **2009**, *37*, 6883.
(5) Liu, P.; Cai, W.; Fang, M.; Li, Z.; Zeng, H.; Hu, J.; Luo, X.; Jing, W. *Nanotechnology* **2009**, *20*, 285707.
(6) Yao, D.; Zhang, G.; Li, B. *Nano Lett.* **2008**, *8*, 4557.
(7) Liu, S.; Yu, J.; Jaroniec, M. *Chem. Mater.* **2011**, *23*, 4085.
(8) Diebold, U. *Surf. Sci. Rep.* **2003**, *48*, 53.
(9) Yang, H. G.; Sun, C. H.; Qiao, S. Z.; Zou, J.; Liu, G.; Smith, S. C.; Cheng, H. M.; Cheng, H. M.; Lu, G. Q. *Nature* **2008**, *453*, 638.
(10) Sun, C.; Liu, L.-M.; Selloni, A.; Lu, G. Q.; Smith, S. C. *J. Mater. Chem.* **2010**, *20*, 10287.
(11) Ramamoorthy, M.; Vanderbilt, D.; King-Smith, R. D. *Phys. Rev. B* **1994**, *49*, 16721.
(12) Swany, V.; Muscat, J.; Gale, J. D.; Harrison, N. M. *Surf. Sci.* **2002**, *504*, 115.
(13) Kröger, E. A.; Sayago, D. I.; Allegretti, F.; Knight, M. J.; Polcik, M.; Unterberger, W.; Lerotholi, T. J.; Hogan, K. A.; Lamont, C. L. A.; Woodruff, D. P. *Phys. Rev. B* **2007**, *75*, 195413.
(14) Pang, C. L.; Lindsay, R.; Thornton, G. *Chem. Soc. Rev.* **2008**, *37*, 2328 and references therein..
(15) Cabailh, G.; Torrelles, X.; Lindsay, R.; Bikondoa, O.; Joumard, I.; Zegenhagen, J.; Thornton, G. *Phys. Rev. B* **2007**, *75*, 241403(R).
(16) Lindan, P. J. D.; Harrison, N. M.; Gillan, M. J.; White, J. A. *Phys. Rev. B* **1997**, *55*, 15919.
(17) Deskins, N. A.; Rousseau, R.; Dupuis, M. *J. Phys. Chem. C* **2010**, *114*, 5891.
(18) Deskins, N. A.; Rousseau, R.; Dupuis, M. *J. Phys. Chem. C* **2011**, *115*, 7562.

(19) Chrétien, S.; Metiu, H. *J. Phys. Chem. C* **2011**, *115*, 4696.

(20) Dohnálek, Z.; Lyubinetsky, I.; Rousseau, R. *Prog. Surf. Sci.* **2010**, *85*, 161.

(21) Lindan, P. J. D.; Harrison, N. M.; Gillan, M. J. *Phys. Rev. Lett.* **1998**, *80*, 762.

(22) Lindan, P. J. D.; Zhang, C. *J. Chem. Phys.* **2003**, *118*, 4620.

(23) Harris, L. A.; Quong, A. A. *Phys. Rev. Lett.* **2004**, *93*, 086105.

(24) Lindan, P. J. D.; Zhang, C. *Phys. Rev. B* **2005**, *72*, 075439.

(25) Wendt, S.; Matthiesen, J.; Schaub, R.; Vestergaard, E. K.; Lægsgaard, E.; Besenbacher, F.; Hammer, B. *Phys. Rev. Lett.* **2006**, *96*, 066107.

(26) Li, S.-C.; Zhang, Z.; Sheppard, D.; Kay, B. D.; White, J. M.; Du, Y.; Lyubinetsky, I.; Henkelman, G.; Dohnálek, Z. *J. Am. Chem. Soc.* **2008**, *130*, 9080.

(27) Bandura, A. V.; Kubichi, J. D.; Sofo, J. O. *J. Phys. Chem. B* **2008**, *112*, 11616.

(28) Valentin, C. D.; Pacchioni, G.; Selloni, A. *Phys. Rev. Lett.* **2006**, *97*, 166803.

(29) Hammer, B.; Wendt, S.; Besenbacher, F. *Top Catal.* **2010**, *53*, 423.

(30) Onda, K.; Li, B.; Zhao, J.; Jordan, K. D.; Yang, J.; Petek, H. *Science* **2005**, *308*, 1154.

(31) Meunier, V.; Pan, M. H.; Moreau, F.; Park, K. T.; Plummer, E. W. *Proc. Natl. Acad. Sci. U.S.A.* **2010**, *107*, 14968.

(32) Peng, H.; Li, J. *J. Phys. Chem. C* **2008**, *112*, 20241.

(33) He, T.; Hu, Z. S.; Li, J. L.; Yang, G. W. *J. Phys. Chem. C* **2011**, *15*, 13837.

(34) Bates, S. P.; Kresse, G.; Gillan, M. J. *Surf. Sci.* **1997**, *385*, 386.

(35) Bredow, T.; Giordano, L.; Cinquini, F.; Pacchioni, G. *Phys. Rev. B* **2004**, *70*, 035419.

(36) Kowalski, P. M.; Meyer, B.; Marx, D. *Phys. Rev. B* **2009**, *79*, 11540.

(37) Kiejna, A.; Pabisiak, T.; Gao, S. W. *J. Phys.: Condens. Matter* **2006**, *18*, 4207.

(38) Mitev, P. D.; Hermansson, K.; Montanari, B.; Refson, K. *Phys. Rev. B* **2010**, *81*, 134303.

(39) Ordejon, P.; Artacho, E.; Soler, J. M. *Phys. Rev. B* **1996**, *53*, R10441.

(40) Sanchez-Portal, D.; Ordejon, P.; Artacho, E.; Soler, J. M. *Int. J. Quantum Chem.* **1997**, *65*, 453.

(41) Soler, J. M.; Artacho, E.; Gale, J. D.; Garcia, A.; Junquera, J.; Ordejon, P.; Sanchez-Portal, D. *J. Phys.: Condens. Matter.* **2002**, *14*, 2745.

(42) Kohn, W.; Sham, L. J. *Phys. Rev.* **1965**, *140*, A1133.

(43) Hohenberg, P.; Kohn, W. *Phys. Rev.* **1964**, *136*, B864.

(44) Kleinman, L.; Bylander, D. M. *Phys. Rev. Lett.* **1982**, *48*, 1425.

(45) Bylander, D. M.; Kleinman, L. *Phys. Rev. B* **1990**, *41*, 907.

(46) Troullier, N.; Martins, J. L. *Phys. Rev. B* **1991**, *43*, 1993.

(47) Ceperley, D. M.; Alder, B. J. *Phys. Rev. Lett.* **1980**, *45*, 566.

(48) Ordejon, P.; Soler, J. M. *Phys. Rev. B* **1996**, *53*, 10441.

(49) Monkhorst, H. J.; Pack, J. D. *Phys. Rev. B* **1976**, *13*, 5188.

(50) Abrahams, S. C.; Bernstein, J. L. *J. Chem. Phys.* **1971**, *55*, 3206.

(51) Mikami, M.; Nakamura, S.; Kitao, O.; Arakawa, H.; Gonze, X. *Jpn. J. Appl. Phys.* **2000**, *39*, 847.

(52) Muscat, J.; Swamy, V.; Harrison, N. M. *Phys. Rev. B* **2002**, *65*, 224112.

(53) Burdett, J. K.; Hughbanks, T.; Miller, G. J.; Richardson, J. W.; Smith, J. V. *J. Am. Chem. Soc.* **1987**, *109*, 3639.

(54) Rasmussen, M. D.; Molina, L. M.; Hammer, B. *J. Chem. Phys.* **2004**, *120*, 988.

(55) Oviedo, J.; San Miguel, M. A.; Sanz, J. F. *J. Chem. Phys.* **2004**, *121*, 7427.

(56) Hameeuw, K. J.; Cantele, G.; Ninno, D.; Trani, F.; Iadonisi, G. *J. Chem. Phys.* **2006**, *124*, 024708.

(57) Henkelman, G.; Arnaldsson, A.; Jónsson, H. *Comput. Mater. Sci.* **2006**, *36*, 254.

(58) Murugan, P.; Kumar, V.; Kawazoe, Y. *Phys. Rev. B* **2006**, *73*, 075401.